A Compact 118-GHz Radiometer Antenna for the Micro-Sized Microwave Atmospheric Satellite

Idahosa A. Osaretin, *Member, IEEE*, Michael W. Shields, *Senior Member, IEEE*, Jose A. Martinez Lorenzo, and William J. Blackwell, *Senior Member, IEEE*

***Abstract*—A linear polarized 118-GHz antenna is designed for a radiometer payload hosted aboard a 3U atmospheric CubeSat. The radiometer antenna is a horn-fed offset parabolic reflector. The antenna has a maximum $+37$ dBi realized gain, 2.4° half-power beamwidth, and a minimum 95% beam efficiency within the operational bandwidth. The antenna is compact, meeting the MicroMAS mission requirement for a highly integrated and ultra-compact radiometer. CubeSats present stringent size/volume and weight constraints on overall component design. We present our design, along with simulated and measured results, that meet the size/volume, weight, and electrical requirements for the radiometer antenna and comply with CubeSat standards.**

***Index Terms*—CubeSat, horn antennas, low Earth orbit satellite, microwave radiometry, radiometers, reflector antennas.**

I. Introduction

THE MICRO-SIZED Microwave Atmospheric Satellite (MicroMAS) is a scalable, CubeSat-based system that addresses the need for low-cost, mission-flexible, and rapidly deployable spaceborne sensors. MicroMAS comprises a complete 3U ($10 \times 10 \times 30$ cm^3) atmospheric sounder, including a 1U ($10 \times 10 \times 10$ cm^3) 118-GHz radiometer payload module developed at MIT Lincoln Laboratory (LL) in collaboration with the UMass-Amherst Department of Radio Astronomy and a 2U spacecraft bus developed by the MIT Space Systems Laboratory in collaboration with MIT Lincoln Laboratory. The 2U ($10 \times 10 \times 20$ cm^2) spacecraft bus includes attitude determination and control, avionics, power, and communications systems. The spacecraft bus also includes a custom scanner-assembly that spins the radiometer payload at 40 r/min about the Space Vehicle's velocity vector, providing cross-track scans as the satellite orbits the earth. The radiometer payload includes highly integrated, ultra-compact, and low-power microwave receivers, electronics, and an antenna that conforms to the CubeSat size, weight, and power standards [1].

Manuscript received May 21, 2014; revised July 02, 2014; accepted July 23, 2014. Date of publication July 25, 2014; date of current version August 12, 2014. This work was supported by the National Oceanic and Atmospheric Administration under Air Force under Contract FA8721-05-C-0002. Opinions, interpretations, conclusions, and recommendations are those of the authors and not necessarily endorsed by the United States Government.

I. A. Osaretin, M. W. Shields, and W. J. Blackwell are with Lincoln Laboratory, Massachusetts Institute of Technology, Lexington, MA 02420 USA (e-mail: Idahosa.Osaretin@ll.mit.edu; shields@ll.mit.edu; wjb@ll.mit.edu).

J. A. Martinez is with the Department of Electrical and Computer Engineering, Northeastern University, Boston, MA 02115 USA (e-mail: jmartine@ece.neu.edu).

Color versions of one or more of the figures in this letter are available online at http://ieeexplore.ieee.org.

Digital Object Identifier 10.1109/LAWP.2014.2343155

Reflector antennas are common in passive microwave radiometer systems [2]. The offset parabolic antenna is an ideal radiometer antenna, as the feed can be connected directly to the radiometer (low losses), and the antenna has suppressed sidelobes, with no aperture blockage present [2]–[6]. The design of a horn-fed offset parabolic reflector is straightforward. However, the mass and volume requirement on the MicroMAS payload places significant constraints on the design. Electrical requirements are the following.

1) The antenna shall have a 2.4° half-power beamwidth (HPBW) in both principal planes.
2) The antenna shall have beam efficiency no less than 95%.
3) The realized gain of the antenna shall be a minimum of $+35$ dBi.
4) The antenna shall have stable pattern and low cross-polarization levels (20 dB isolation) performance across the frequency band 108–120 GHz.

Mechanical design constraint is that the antenna subsystem fits a 0.5U ($10 \times 10 \times 5$ cm^3) volume and balances out the mass of the radiometer to maintain a center of gravity (CG) within 1.3 mm of the payload spin axis. Section II presents the antenna design, and Section III presents the performance characterization of the linearly polarized horn-fed offset parabolic reflector antenna for the MicroMAS radiometer payload.

II. Antenna Design

Our design centered on a high-gain offset-fed parabolic reflector antenna. A corrugated horn feed is optimal to ensure suppressed sidelobes and symmetric beam radiation patterns [6]–[10]. Finally, we designed a reflector shroud to limit multipath interference within the payload. The design parameters for the reflector, horn feed, and shroud are as follows.

A. Reflector

The reflector aperture diameter is constrained by the size of the payload. The maximum possible aperture diameter (D) of 8 cm is used. The offset angle and height of center for the parabolic reflector are minimized to reduce cross-polarization response [3], [6]. The reflector height of center (H) is designed as 4.5 cm. The reflector focal length (f) is constrained by the mechanical/volume requirements; hence we designed the f/D ratio as 0.56. The reflector half-cone angle (ψ_e) is 40.18°, and the feed is pointed at angle $\psi_f = 50.55°$ toward the center of the reflector to reduce feed spillover. An 18.4-dB edge taper is implemented in the horn design for high aperture efficiency and to obtain low phase variation across the reflector [3]. An image

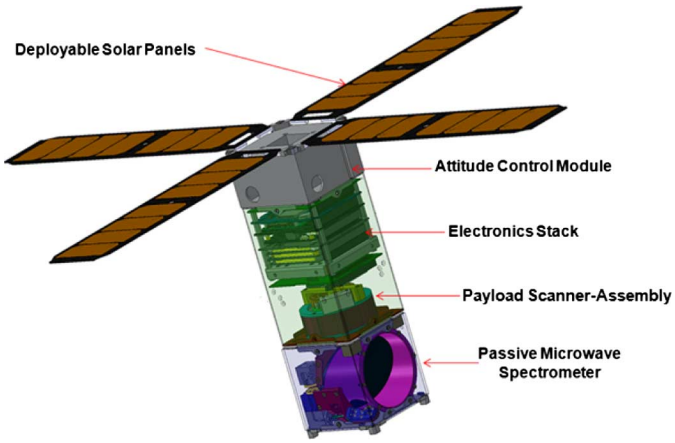

Fig. 1. Computer-aided design (CAD) rendition of the MicroMAS space vehicle.

Fig. 2. Front and rear views of the fabricated MicroMAS radiometer antenna.

of the reflector antenna, as built, is shown in Fig. 2. Design and analysis of the reflector uses TICRA GRASP.

B. Corrugated Horn

In corrugated horn designs, the aperture, corrugations, flare section, and throat design parameters are critical to ensure desired performance [7], [8], [10]. The horn aperture diameter and flare angle are key parameters that control copolar radiation characteristics; the throat and corrugation design parameters control cross-polarization characteristics [7], [10]. To meet the mechanical and electrical requirements for the antenna, the horn flare angle was designed as $7.25°$, aperture diameter as 1.12λ, input waveguide diameter as 0.5λ, corrugation slot width of 0.15λ, corrugation ridge-to-slot ratio of 0.5, with slot depths of 0.5λ at the throat tapering to 0.24λ at the aperture, and an overall horn length of 4.8λ, where λ is the free-space wavelength at 118 GHz. The corrugations are designed such that the slot depth at the throat of the horn was a half-wavelength at the maximum frequency and the slot depth at the aperture was a quarter-wavelength at the center of the operational frequency band.

C. Reflector Shroud

We designed a reflector shroud for the radiometer payload to minimize interference resulting from multipath reflection within the payload and control possible spillover from the corrugated horn [11]. The shroud creates a collimated volume around the reflector, negating multipath interference. The conducting reflector shroud also functioned as a ballast, to keep the CG of the radiometer payload within 1.3 mm (spacecraft attitude control requirement) of the payload spin axis. The shroud's internal diameter was designed as 8 cm to fit the reflector aperture. The numerical model of the reflector antenna with conducting shroud generated is shown in Fig. 3. The design analysis considered a conducting shroud with three different internal surfaces—a smooth wall, a roughened wall, and a smooth wall coated with low-loss dielectric material. The analysis determined the effect of the shroud and each internal surface type on the overall radiation pattern, with focus on the radiation beam efficiency.

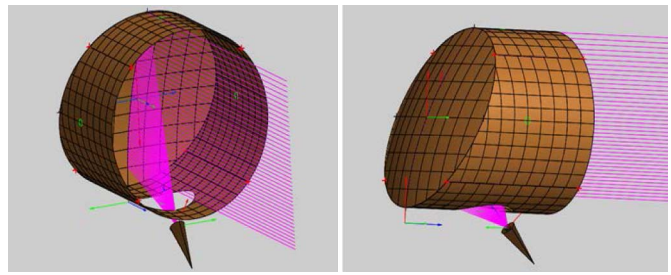

Fig. 3. TICRA GRASP simulation model of the MicroMAS reflector antenna complete with the reflector shroud.

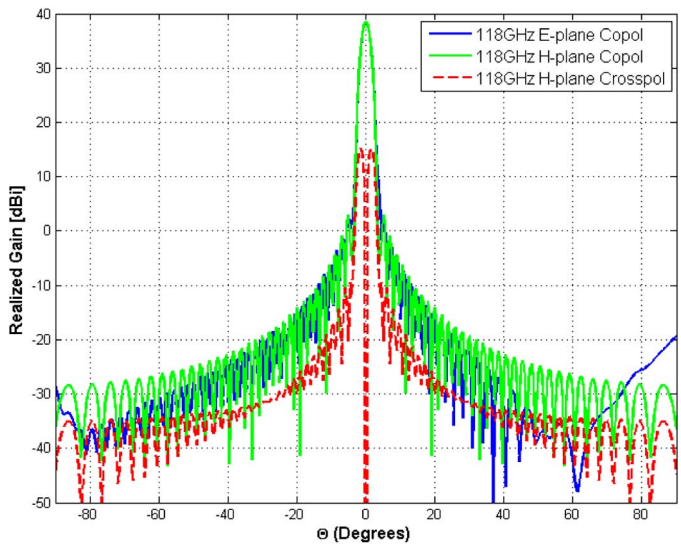

Fig. 4. Simulated radiation pattern for the radiometer antenna without the reflector shroud. The cross-polarization pattern in the E-plane is below the range displayed and is not plotted.

III. Antenna Analysis and Results

Numerical simulation and optimization of the corrugated horn feed was done using ANSYS HFSS. The horn feed design optimization included design of the corrugations (slot width, slot depth, and ridge-to-sloth ratio), aperture, and overall horn length. Upon completion of the horn design, the resulting antenna pattern data were exported to TICRA GRASP for reflector antenna analysis. The numerical analysis of the reflector antenna is based upon physical optics (PO), complemented with physical theory of diffraction (PTD). Simulated radiation pattern from the horn-fed reflector antenna model is shown in Fig. 4. The pattern shown in Fig. 4 includes only the reflector

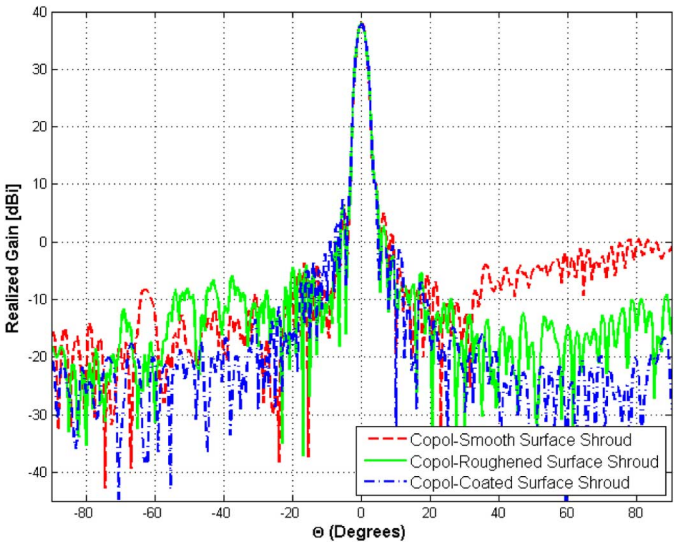

Fig. 5. Simulated E-plane radiation pattern for the smooth, roughened, and coated interior surface of the shroud. Better sideblobe levels are observed for the roughened and coated surfaces.

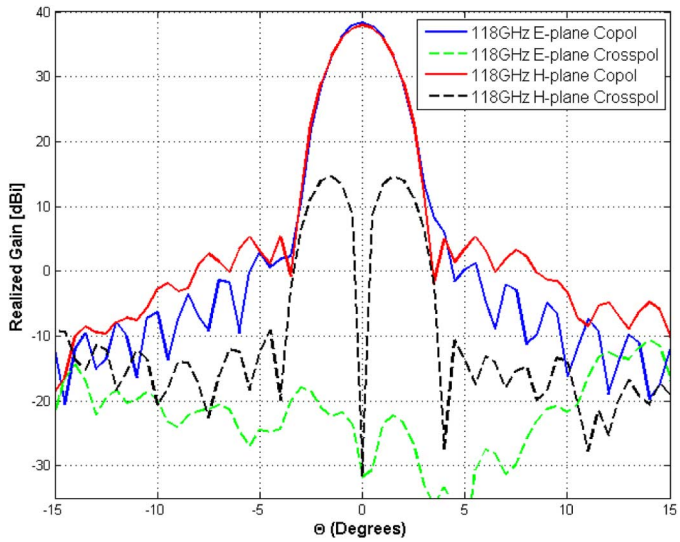

Fig. 6. Simulated copolar and cross-polar gain patterns of antenna assembly with shroud (as shown in Fig. 3).

and horn feed. The pattern shows high antenna gain, +25 dB cross-polarization isolation, and low sidelobes. The HPBW is computed as 2.39°, and the beam efficiency as 99%. Here, the beam efficiency is computed as the ratio of the power within the antenna's main lobe (defined as 2.5 times the HPBW) and the total transmitted power of the antenna. The results met the antenna requirements, and the reflector antenna was ready for fabrication. The parabolic reflector was fabricated with a surface tolerance of 0.001 cm root mean square (RMS). Measurements of the antenna as shown in Fig. 2 were made to verify design and fabrication accuracy.

Numerical simulation of the reflector shroud, for all three internal surface cases, was implemented using TICRA GRASP. The roughened surface was modeled as a 0.5-mm maximum peak random surface error ($RMS = 0.24 \times \text{peak}$) on the internal shroud wall. The roughness is modeled as rapidly varying errors, which scatter the incident field into a wide angular region but at very low amplitude [12]. The analysis considered two possible field contributions to the radiation pattern: 1) field contributions due to spillover radiation from the corrugated horn that is scattered by the shroud and illuminates the reflector; and 2) field contributions due to scattered fields from the reflector edge that reflects off the shroud and into the far-field pattern. The numerical analysis used PO and PTD for the reflector and method of moments (MoM) for the conducting shroud.

Simulated radiation pattern for the shroud analysis is shown in Fig. 5. The results show no impact on the HPBW, with beam efficiencies for the smooth, roughened, and coated surface, respectively as 92%, 97%, and 98%. We decided to proceed with the roughened surface due to outgassing concerns with a dielectric coat. Copolar and cross-polar simulated radiation patterns for the roughened shroud surface are shown in Fig. 6. We observe a stable beam with greater than +20 dB cross-polarization isolation and low sidelobe levels. Upon completion of this analysis, the reflector shroud was fabricated with the interior surface sandblasted to a fine finish.

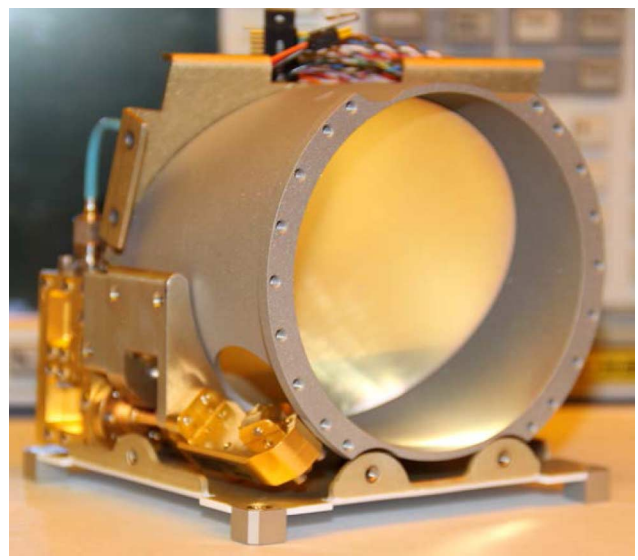

Fig. 7. MicroMAS radiometer antenna subsystem with the roughened-wall reflector shroud integrated.

The radiometer antenna was integrated as shown in Fig. 7. Measurements of the radiometer antenna, complete with the reflector shroud, were made at the MIT LL Compact Antenna Test Range (CATR). The measurements are taken across the radiometer operational frequency band, with the antenna in the configuration shown in Fig. 7. Radiation pattern plots from the measurements are shown in Fig. 8. At 108 GHz, results show HPBWs of 2.47° in the E-plane and 2.50° in the H-plane. At 113 GHz, HPBWs of 2.38° in the E-plane and 2.44° in the H-plane were obtained. At 118 GHz, results show HPBWs of 2.30° in the E-plane and 2.37° in the H-plane. Offsets observed in the antenna boresight direction in Fig. 8 are due to displacement of the feedhorn phase center, per frequency, from the reflector focal point.

Results show that the measured antenna characteristics meet the design requirements across the operational frequency band in terms of the cross-polarization isolation (greater than +20 dB

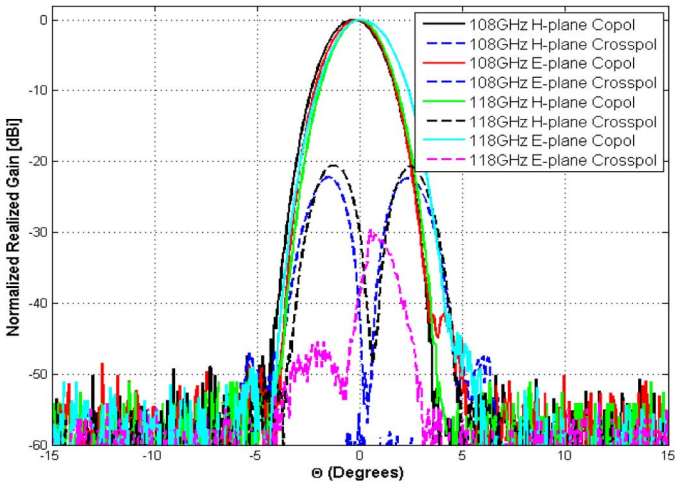

Fig. 8. Measured radiation pattern of antenna assembly with shroud (as shown in Fig. 7). Copolar and cross-polar characteristics are shown.

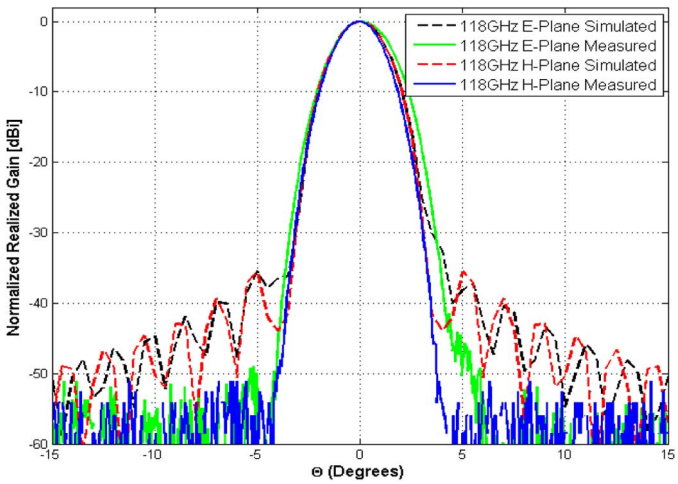

Fig. 9. Comparison of measured and simulated antenna gain patterns for E- and H-planes, showing good agreement.

in Fig. 8) and gain. Beam efficiency computations were not carried out on the measured data due to problems detecting the sidelobe pattern in the noise floor of the MIT LL CATR. Hence, we relied on beam efficiency computations from the simulated antenna patterns. To ensure that the simulated patterns gave reliable approximations of the measured results, we compared the simulated and measured pattern data. A comparison of the simulated antenna radiation pattern and the measured antenna radiation pattern is shown in Fig. 9. The results show good agreement in the main boresight lobe. However, the lateral sidelobes in the measured pattern are absent due to technical limitations during measurements.

IV. Conclusion

The antenna meets all design specifications, delivering +37 dBi of realized gain with better than +20 dB cross-polarization isolation in the E-plane, H-plane, and 45° planes. The antenna subsystem met the mechanical/volume constraints, allowing the CG of radiometer payload to meet the design specification. The radiometer antenna was integrated into the MicroMAS payload and successfully completed radiometer calibration testing under thermal vacuum. The MicroMAS Space Vehicle, shown in Fig. 10, successfully completed functional and environmental testing at MIT LL's Environmental Test Laboratory and launched aboard the Cygnus Orb-2 ISS Resupply Mission in July 2014.

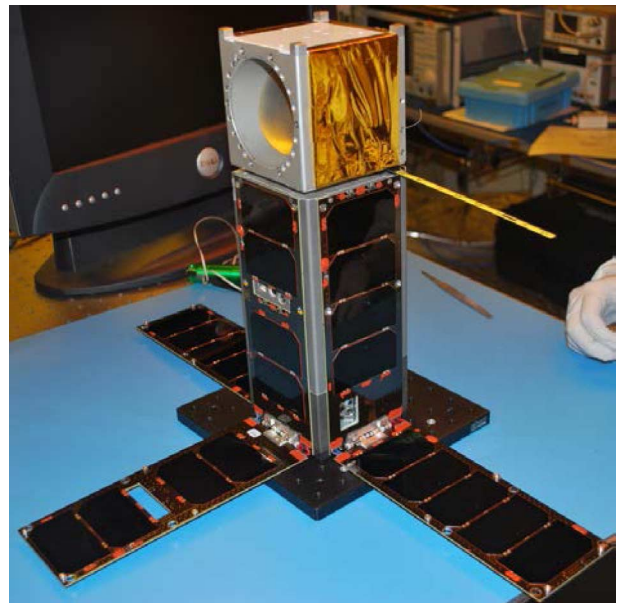

Fig. 10. Integrated MicroMAS Space vehicle.

Acknowledgment

The authors wish to acknowledge Millitech, Inc., of Northampton, MA, USA, for the structural redesign, fabrication, and initial measurements of the MicroMAS radiometer antenna.

References

[1] California Polytechnic State University, San Luis Obispo, CA, USA, "CubeSat design specification," Rev. 13, 2014.
[2] N. Skou, *Microwave Radiometer Systems: Design and Analysis*. Norwood, MA, USA: Artech House, 1989.
[3] T. A. Milligan, *Modern Antenna Design*, 2nd ed. Hoboken, NJ, USA: Wiley, 2005.
[4] A. W. Rudge and N. A. Adatia, "Offset-parabolic-reflector antennas: A review," *Proc. IEEE*, vol. 66, no. 12, pp. 1592–1618, Dec. 1978.
[5] P. A. Venkatachalam, N. Gunasekaran, and K. Raghavan, "An offset reflector antenna with low sidelobes," *IEEE Trans. Antennas Propag.*, vol. AP-33, no. 6, pp. 660–662, Jun. 1985.
[6] S. B. Sharma, D. Pujara, S. B. Chakrabarty, and R. Dey, "Cross-polarization cancellation in an offset parabolic reflector antenna using a corrugated matched feed," *IEEE Antennas Wireless Propag. Lett.*, vol. 8, pp. 861–864, 2009.
[7] X. Zhang, "Design of conical corrugated feed horns for wide-band high-frequency applications," *IEEE Trans. Microw. Theory Tech.*, vol. 41, no. 8, pp. 1263–1274, Aug. 1993.
[8] G. James, "Design of wide-band compact corrugated horns," *IEEE Trans. Antennas Propag.*, vol. AP-32, no. 10, pp. 1134–1138, Oct. 1984.
[9] B. Berkowitz, "Antennas fed by horns," *Proc. IRE*, vol. 41, no. 12, pp. 1761–1765, Dec. 1953.
[10] P. J. B. Clarricoats and A. D. Olver, *Corrugated horns for Microwave Antennas*. London, U.K.: Peregrinus, 1984.
[11] H. P. Coleman, R. M. Brown, and B. D. Wright, "Paraboloidal reflector offset fed with a corrugated conical horn," *IEEE Trans. Antennas Propag.*, vol. AP-23, no. 6, pp. 817–819, Nov. 1975.
[12] TICRA Engineering Consultants, Copenhagen, Denmark, "GRASP technical description," 2008.